Journal of Energy and Power Engineering 10 (2016) 425-430
doi: 10.17265/1934-8975/2016.07.006

# A Numerical Method for Calculating Interior Ballistics of Electrothermal Accelerator

Aleksey A. Vorobiev

*Scientific Innovation Center of Rocket and Space Technologies, Kitaygorodskiy 9, Moscow 109074, Russia*

Received: May 03, 2016 / Accepted: May 16, 2016 / Published: July 31, 2016.

**Abstract:** Electro-thermal accelerator uses high-voltage arc energy to heat the actuating medium, it being made from low-molecular weight material. Projectile acceleration is achieved by expansion of the actuating medium. Numerical method for calculating interior ballistics uses Lagrangian coordinates there the conservation of momentum and the energy balance are solved. A statement of the energy balance reflects the second law of thermodynamics. Lagrangian different grid and scheme for numerical calculation were used. Fully explicit scheme was employed. The solving includes two stability conditions: Courant and shock (artificial viscosity). Numerical results were compared with the experimental research for pressure in the barrel in electro-thermal accelerator.

**Key words:** Electro-thermal accelerator, plasma, capacitor, discharge chamber.

## 1. Introduction

ETA (electro-thermal accelerator) uses high-voltage arc energy to heat the actuating medium, it being made from low-molecular weight material. Projectile acceleration is achieved by expansion of the actuating medium. ETA structure, operating principle and some results are presented in Refs. [1, 2]. The process in the ETA discharge chamber is similar with an explosion because of extremely high current and short time (Fig. 1).

A description of the dynamics of an explosion can be obtained from the solution of a set of nonlinear, partial differential equations which represent the conservation of mass, momentum, and energy in some symmetry.

## 2. Mathematical Formulation

In terms of the variables explicitly treated in this calculation, the expression of the conservation of the mass takes the following differential form:

$$V(x,t)=\frac{1}{\rho(x,t)}=\frac{\partial \mathrm{X}(x,t)}{\partial m} \tag{1}$$

where, $\rho$ represents density, $V$ represents specific volume, $X$ represents spatial dimension, $m$ represents the mass. The conservation of momentum in differential form appears as

$$\frac{\partial u}{\partial t}=-\frac{\partial}{\partial m}(P+Q) \tag{2}$$

where, $u(x,t)=\frac{\partial \mathrm{X}(x,t)}{\partial t}$ is a particle or gas velocity, $P$ is pressure, $Q$ is the artificial viscosity pressure, $X(x, t)$ represents eulerian coordinate, $x$ is Lagrangian coordinate, $m(x,t)=\int_0^x \rho(x,t)dx$ represents mass in plane symmetry.

The artificial viscosity form in plane geometry considered by Ref. [3] was

$$Q(x,t)=\begin{cases}\dfrac{C_1(\Delta m)^2}{V}\left|\dfrac{\partial V}{\partial t}\right|^2+\dfrac{C_2\cdot\Delta m}{V}\left|\dfrac{\partial V}{\partial t}\right|, & \text{at } \dfrac{\partial V}{\partial t}<0,\\ 0, & \text{at } \dfrac{\partial V}{\partial t}\geq 0,\end{cases} \tag{3}$$

**Corresponding author:** Aleksey A. Vorobiev, Ph.D., associated professor, research fields: physics of extreme states of matter, laser technics and technologies.

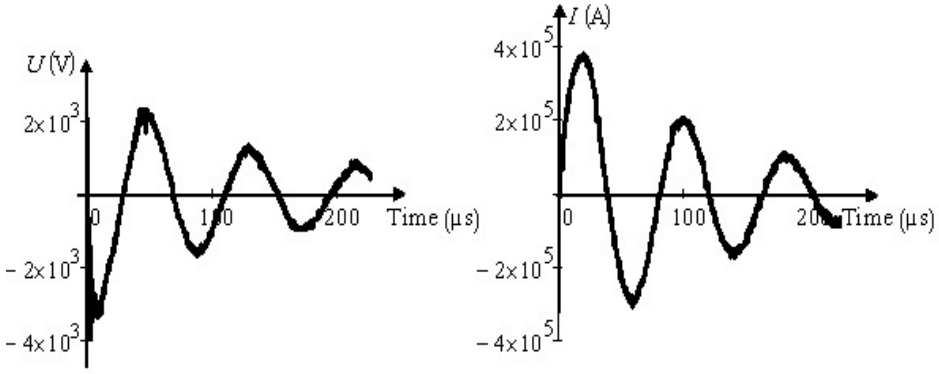


**Fig. 1 Voltage and current in the discharge chamber.**

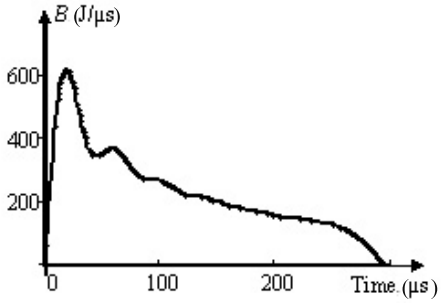


**Fig. 2 Energy input rate in the ETA discharge chamber.**

where, $C_1$ and $C_2$ are arbitrary constants, dimensionless and of values near unity. A statement of the energy balance in differential form reflects the second law of thermodynamics:

$$\frac{\partial \mathrm{E}}{\partial t} = -(P+Q)\frac{\partial \mathrm{V}}{\partial t} + B(t) \tag{4}$$

The *B*-term symbolizes an energy input rate. In the case of ETA *B*-case term is the energy of high-voltage arc in the discharge chamber versus time (Fig. 2).

## 3. Difference Equations

Lagrangian different grid (Fig. 3) and scheme for numerical calculation were used as in Ref. [3].

Fig. 3 denotes the particular choice of notation and concentration of variables at mass points and time points.

The mass is identified with the half points in the "*j*" variables, the time is centered at the half points in the "*n*" variables, and the various quantities such as the velocities, radii, specific volumes, pressures, and energies are identified at the time and mass points indicated in the diagram. With such an identification it is possible to translate the differential equations into difference equations which largely deal with centered quantities. That is, each difference equation is balanced about the same time point and the same mass point in order to avoid first order numerical errors in the approximation of differentials by finite differences. A common procedure is to begin as in equations listed below [3], to develop at time $n + 1$ a new velocity and then to find a new radius $X$ for each $j$ point. From the new radii one can define a new density or specific volume, and from the change in density, an artificial viscosity at the new time.

First:

$$u_j^{n+1/2} = u_j^{n-1/2} - \frac{\Delta t}{\Delta m}\left[P_{j+1/2}^n - P_{j-1/2}^n + Q_{j+1/2}^{n-1/2} - Q_{j-1/2}^{n-1/2}\right] \tag{5}$$

then

$$X_j^{n+1} = X_j^n + u_j^{n+1/2}\frac{\Delta t}{2} \tag{6}$$

and

$$V_{j-1/2}^{n+1} = \frac{X_j^{n+1} + X_{j-1}^{n+1}}{0.5\cdot\Delta m} \tag{7}$$

The artificial viscosity becomes

$$Q_{j-1/2}^{n+1/2} = \frac{C_1(\Delta m)^2\left(V_{j-1/2}^{n+1} - V_{j-1/2}^n\right)^2}{\left(V_{j-1/2}^{n+1} + V_{j-1/2}^n\right)(0.5\cdot\Delta t)^2} + \frac{C_2\Delta m\left|V_{j-1/2}^{n+1} - V_{j-1/2}^n\right|}{\left(V_{j-1/2}^{n+1} + V_{j-1/2}^n\right)0.5\cdot\Delta t} \tag{8}$$

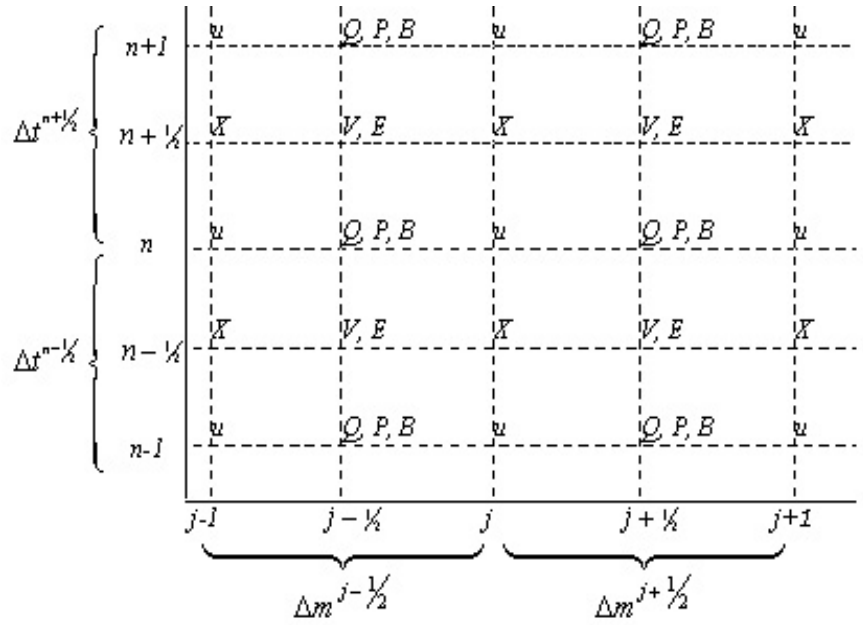


**Fig. 3 Lagrangian different grid.**

for $V^{n+1} < V^n$, and $Q_{j-\frac{1}{2}}^{n+\frac{1}{2}} = 0$ for $V^{n+1} \geq V^n$. For hydrodynamics only, the energy equitation can be written as Ref. [3]:

$$E_{j-\frac{1}{2}}^{n+1} = E_{j-\frac{1}{2}}^{n} - \left[P_{j-\frac{1}{2}}^{n+\frac{1}{2}} + Q_{j-\frac{1}{2}}^{n+\frac{1}{2}}\right]\left(V_{j-\frac{1}{2}}^{n+1} - V_{j-\frac{1}{2}}^{n}\right) + B_{j-\frac{1}{2}}^{n+\frac{1}{2}} \tag{9}$$

where,

$$P_{j-\frac{1}{2}}^{n+\frac{1}{2}} = E_{j-\frac{1}{2}}^{n}\rho_{j-\frac{1}{2}}^{n}\frac{0.09 + \left(\rho_{j-\frac{1}{2}}^{n}\right)}{0.3 + \left(\rho_{j-\frac{1}{2}}^{n}\right)^2} \tag{10}$$

Fully explicit scheme was employed. The solution includes two stability conditions: Courant and shock (artificial viscosity $Q$). The usual Courant Condition is simply a statement that the time steps should be smaller than the time for a sound signal to propagate beyond the boundaries of adjacent zones. The stability condition can be expressed as

$$\Delta t \leq \Delta m\sqrt{\frac{V}{\gamma \cdot P}} \tag{11}$$

The shock condition is

$$\Lambda = \frac{C_2\Delta t}{X_j^{n+\frac{1}{2}} - X_{j-1}^{n+\frac{1}{2}}} + 8C_1\frac{\left|V_{j-\frac{1}{2}}^{n+1} - V_{j-\frac{1}{2}}^{n}\right|}{\left(V_{j-\frac{1}{2}}^{n+1} + V_{j-\frac{1}{2}}^{n}\right)} \leq 1 \tag{12}$$

where, $C_1 = 6$, $C_2 = 0.5$.

## 4. Numerical Calculating Results

As a result, we achieve pressure, temperature, mass velocity and density versus time and barrel length. For example pressure and mass velocity versus time are shown in Figs. 4-7.

Figs. 4-6 give pressure in linear and logarithmic scales for better visualization. In Figs. 4-7 curves 1-5 describe the field not far from the discharge gap but curves under numerals more than five are the points through the barrel length. Also pressure and mass velocity as a function of the barrel length are presented in Figs. 8 and 9.

## 5. Experiment and Theory

To validate theoretical issues the experiment research was conducted. Fig. 10 gives the experiment scheme.

In Fig. 10, the items are: 1—ETA, 2—capacitor (300 μF, up to 20 kV), 3—vacuum discharge switcher, 4 and 5—electrodes, 6—discharge initiator, 7—actuating medium, 8—projectile, 9—current sensor (contactless magnetic probe), 10—voltage sensor (high-voltage ohm splitter), 11—piezoelectric pressure sensor.

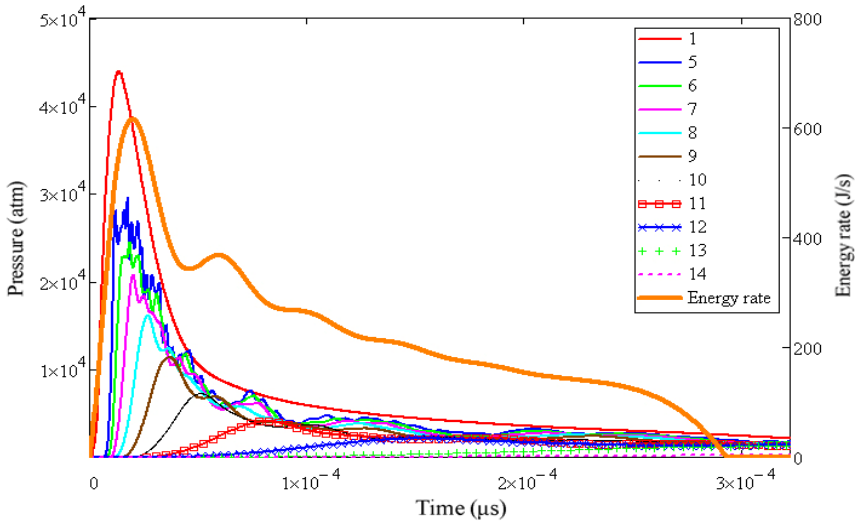


**Fig. 4 Pressure as a function of time for different barrel sections.**

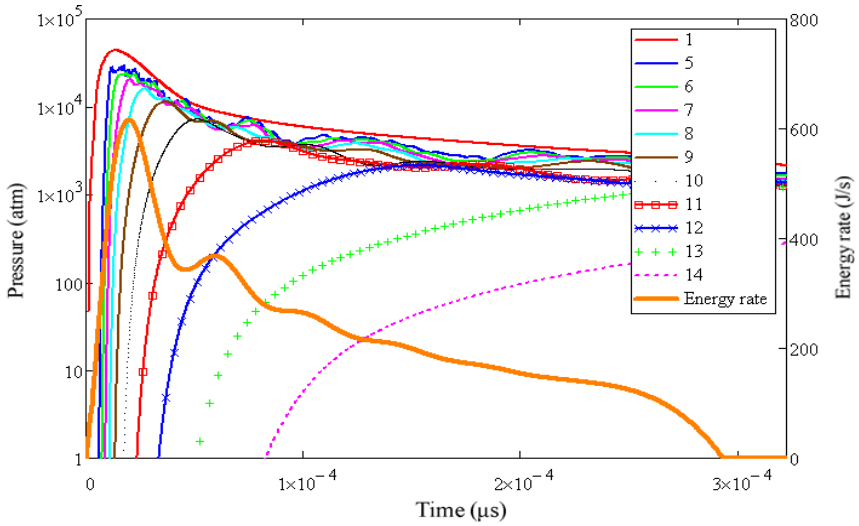


**Fig. 5 Pressure as a function of time (logarithmic scale for ordinates) for different barrel sections.**

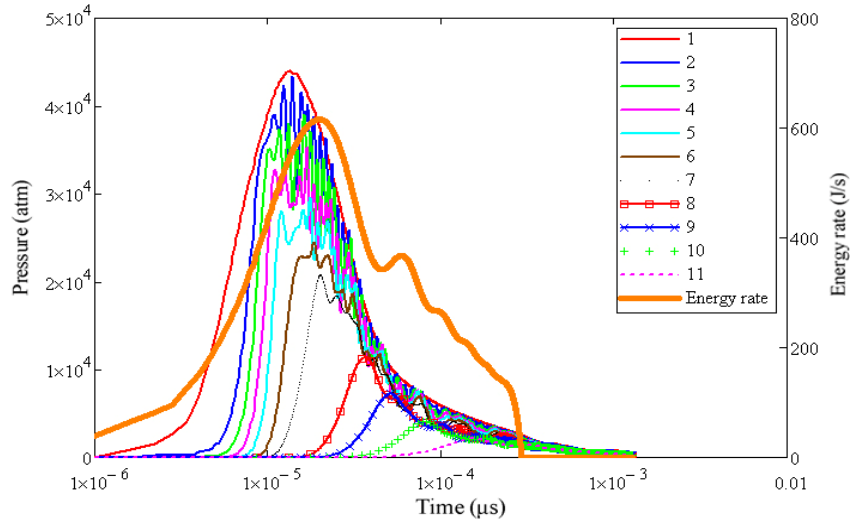


**Fig. 6 Pressure as a function of time (logarithmic scale for abscissas) for different barrel sections.**

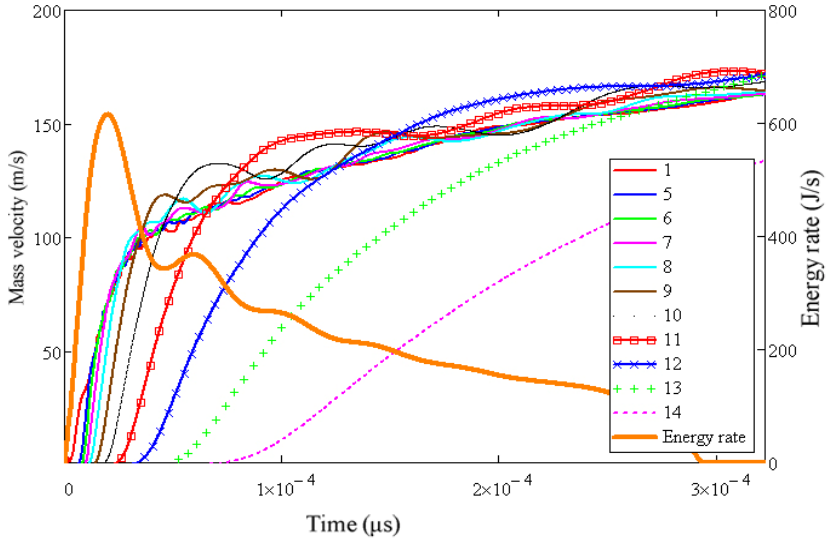


**Fig. 7 Mass velocity as a function of time for different barrel sections.**

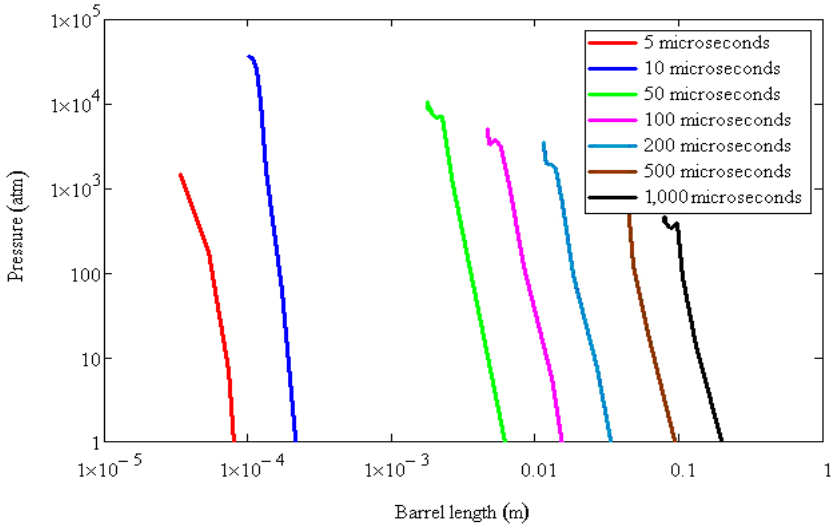


**Fig. 8 Pressure as a function of the barrel length for different times.**

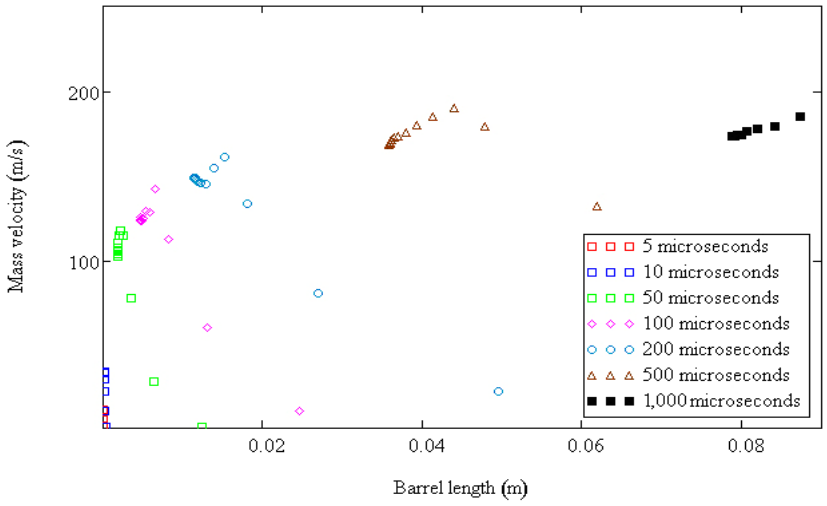


**Fig. 9 Mass velocity as a function of the barrel length for different times.**

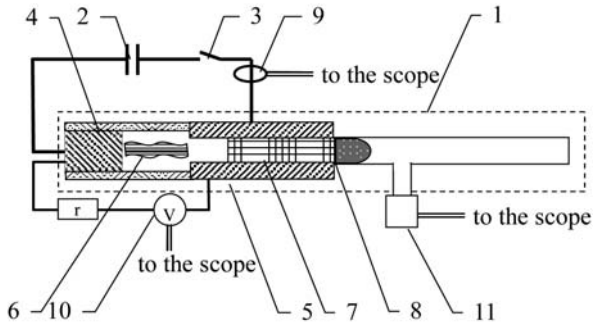


**Fig. 10 Experiment scheme.**

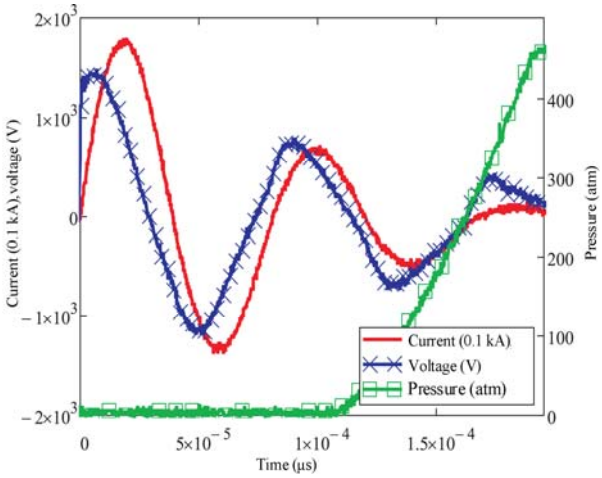


**Fig. 11 Experiment results.**

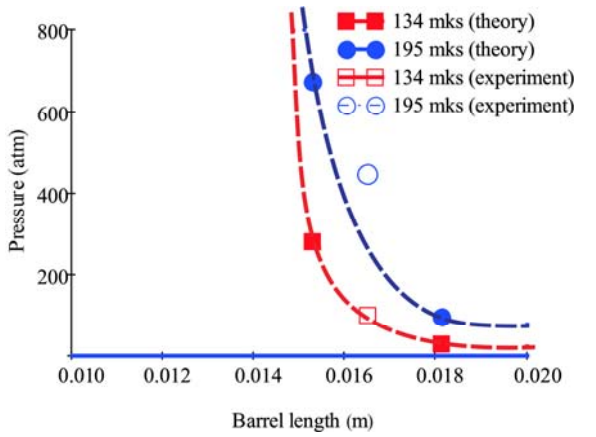


**Fig. 12 Experiment and theory.**

The pressure in the barrel is evaluated in 500 atm then capacitor at 10 kV is discharged (Fig. 11).

The mathematic model gives approximately the same values for the time from 100 to 200 μs and for the same projectile position as it is shown in Fig. 12.

The difference is due to value 5/3 used in numerical calculations. This value depends on the materials used and their equation of the state. For the dense gases of detonation products before expansion or for solids at high temperatures and densities the maximum can exceed 5/3. The value of should be chosen with that in mind. Also the radiation diffusion and added mass was not included in the system of equations solved here.

## 6. Conclusions

Relative mathematical model was created for exploration of interior ballistics in elector-thermal accelerator. Simply, if one knows parameters of *R-L-C* circuit it would be possible to evaluate the projectile speed. Further it will be allowed to optimize ETA construction in means of barrel length and electric current shape and duration to achieve the maximum projectile speed and better energy usage.

## Acknowledgments

The research was conducted under financial support of Ministry of Education and Science of Russian Federation within the bounds of President's Grant MK-5250.2016.8.

## References

[1] Spitsin, D. D., Zikova, T. S., Vorobiev, A. A., Komarov, I. S., Chichaeva, O. V., and Trunilin, I. B. 2013. "Development of Two-Stage Electro-Thermal Way to Accelerate Solid Bodies." *Physics of Extreme States of Matter—2013: Joint Institute for High Temperatures of the Russian Academy of Sciences,* 72-4.

[2] Sakharov, M. V., Vorobiev, A. A., Utkin, A. V., Feldshtein, V. A., and Komarov, I. S. 2015. "Automation of the Electro-Thermal Accelerator Processing Experimental Test Bench." *Electromechanical Matters Journal* 144 (1): 36-42.

[3] Brode, H. L., Asano, W., Plemmons, M., Scantlin, L., and Stevenson, A. 1967. *A Program for Calculating Radiation Flow and Hydrodynamics*. Santa Monica: The RAND Corporation.